

1 **Improving knife milling performance for biomass preprocessing by using advanced blade**
2 **materials**

4 **ABSTRACT REFERENCE NUMBER: WEAR2023_0189**

6 Tomas Grejtak¹, Jeffrey A. Lacey², Miranda W. Kuns², Damon S. Hartley³, David N.
7 Thompson⁴, George Fenske⁵, Oyelayo O. Ajayi⁵, Jun Qu^{1,*}

8 ¹Materials Science and Technology Division, Oak Ridge National Laboratory, Oak Ridge, TN
9 USA

10 ²Biological and Chemical Processing Department, Idaho National Laboratory, Idaho Falls, ID
11 USA

12 ³Operations Research and Analysis, Idaho National Laboratory, Idaho Falls, ID USA

13 ⁴Biomass Characterization, Idaho National Laboratory, Idaho Falls, ID USA

14 ⁵Applied Materials Division, Argonne National Laboratory, Lemont, IL USA

16 **Abstract**

17 Mechanical preprocessing of biomass, including size reduction, is a crucial step in converting
18 biomass into biofuel. However, the feedstock inevitably contains abrasive intrinsic and extrinsic
19 inorganics that may cause excessive tool wear in preprocessing. This work demonstrates that the
20 performance of a knife mill can be significantly improved by applying a more wear-resistant
21 blade material. A series of full-scale knife mill testing were performed for size reduction of
22 forest residue using blades of tungsten carbide (WC-Co), iron-borided tool steel, and diamond-
23 like carbon (DLC) coated tool steel. Blade material loss was quantified in correlation to the
24 amount of feedstock processed and wear mechanisms were investigated via worn surface
25 characterization. While the thin DLC coating was removed quickly, the WC-Co and iron-borided
26 blades improved the tool life by 8X and 3X compared with the M2 tool steel blades (baseline),
27 respectively, when compared with the commonly used tool steel blades. In addition, the in-situ
28 throughput and power consumption measurements provided additional insights. The WC-Co and
29 iron-borided blades maintained ~3X higher throughput than the baseline blades by the end of the
30 test with lower normalized power consumption. The experimental results were then used as input
31 for a techno-economic analysis, which demonstrated that the more wear resistant blades could
32 reduce the knife milling cost by \$2-3 per ton of biomass processed with downtime reduced by
33 65-85%.

34 **Keywords**

35 biomass size reduction, knife mill, blade wear, throughput

37 **Corresponding Author**

38 Jun Qu

39 phone: (865) 576-9304

40 email: qujn@ornl.gov

42 **Nomenclature**

43		
44	gap_o	initial gap distance in mm;
45	gap_i	evolving gap distance in mm;
46	d	blade edge recession in mm;
47	V_{loss}	volume loss of the blade tip in mm^3 ;
48	ar	wear recession of a rotary blade in mm;
49	as	wear recession of a stationary blade in mm;
50	θ	blade tip angle in degrees;
51	w	blade width in mm;
52	V_r	volume loss of the rotary blade tip in mm^3 ;
53	V_s	volume loss of the stationary blade tip in mm^3 ;
54	A_u	blade tip area of the unworn blade in mm^2 ;
55	A_w	blade tip area of the worn blade in mm^2 ;
56	A	worn blade tip area in mm^2 ;
57	x	blade tip region used for determination of the worn area A in mm;
58	Z_u	height of the unworn blade tip along a region x in mm;
59	Z_w	height of the worn blade tip along a region x in mm;
60		
61		
62		
63		
64		

65 **1. Introduction**

66 Biomass is a renewable source of energy that has a potential to reduce dependency on fossil
 67 fuels and, overall, positively impact the environmental sustainability[1–3]. The most common
 68 sources of biomass-derived energy are agricultural plants, forest residues, microalgae and
 69 municipal solid waste[3–5]. The biggest challenges that bio-energy faces in expansion include
 70 lowering the production cost and increasing in productivity[2].

71 Mechanical biomass preprocessing, such as size reduction, is an important step in converting
 72 biomass into biofuel[6]. Reducing biomass size results in densification which improves its
 73 handling, packing, transportation and biodegradability [7]. Traditionally, gridding of biomass is
 74 enabled by specialized mills such as knife mill, hammer mill, ball mill, attrition mill or
 75 shredders[6], [8]. These pre-processing tools have certain advantages and disadvantages. Hammer
 76 mills offer specific benefits such as low cost or ability to process a wide range of biomass
 77 feedstock, however, they are not suitable for biomass with high moisture[9], [10]. Ball mills have
 78 been shown to be effective in preprocessing the biomass for fermentation and pyrolysis by
 79 decreasing the crystallinity of cellulose[11], [12] although controlling the particle size can be
 80 challenging[13]. Significant research efforts have focused on optimizing shredders. A new rotary
 81 bypass shear mill (Crumbler™) developed by Forest Concepts, LLC significantly reduces the
 82 power consumption and is well adapted for high moisture biomass[6], [14]. Disadvantages of
 83 rotary bypass shear mill are relatively low throughput and inability to reduce the biomass to <
 84 1mm[6]. Knife mill is also used for biomass commination due to its favorable characteristics
 85 such as lower power consumption[15], improved particle flowability and narrower size
 86 distribution[16]. It is typically utilized for biomass with a moisture up to 15%[8]. In a knife mill,
 87 the biomass is ground by a shearing action between stationary and rotary knives[8] and the
 88 milling performance depends on many factors such as the number of knives, milling speed,
 89 particle size requirements, clearance (gap) between knives, and knife bevel angle[17], [18].
 90 However, critical components of a knife mill are subjected to a high wear and damage caused by
 91 inorganic contaminants contained in biomass called ash [19]. These inorganics could either be an
 92 inherent part of biomass as they are contained inside of plants cell (intrinsic ash) or introduced
 93 by soil contaminant (extrinsic ash) during harvesting[20]. Studies showed that feedstock
 94 containing a high concentration of ash causes an excessive wear and damage of a ring and roller
 95 in ring die mills[21], screw press in briquetting extruder[22], grinder blades in hammer mills[10]
 96 and cutters in rotary shear comminution systems[14]. Comprehensive characterization of biomass
 97 ash by Lee et al.[23] revealed that the inorganic particles are dominated by quartz and their size
 98 ranges from smaller particles of ~tens of microns to larger particles of ~hundreds of microns.
 99 Experimental work by Lacey et al.[19] demonstrated that the wear of steel material increases
 100 with increasing ash content. Several methods have been developed to remove the ash from the
 101 biomass in order to minimize the impact of the inorganics on wear and damage of pre-processing
 102 tools such as mechanical separation (size separation and air classification) or chemical
 103 preprocessing (dilute acid leaching or water washing)[20]. However, additional biomass
 104 preprocessing increases the overall operation cost.

105 This paper demonstrates that the performance and durability of a knife mill for biomass
 106 preprocessing can be significantly enhanced by applying wear resistant blade materials. Our
 107 comprehensive analysis of the experiments performed on Eberbach knife mill include wear
 108 mechanisms of candidate blades, biomass particle size distribution, feedstock throughput, and
 109 power consumption. Moreover, a techno-economic analysis was conducted to elucidate the

110 economic benefits from utilizing the advanced blade materials. This work demonstrates that
 111 applying more wear resistant blade materials significantly improves the durability and the
 112 performance of a knife milling operation and the findings from this work could be used as
 113 guidelines for improving the efficiency and reducing the cost for biomass preprocessing.
 114

115 **2. Materials and methods**

116 **2.1. Knife material**

117 In order to select candidate materials for knife mill blades, bench-scale abrasive wear testing
 118 was conducted on a variety of steel alloys, composites, coatings, and surface treatments using the
 119 standard ASTM G174 loop abrasion test [24]. The results showed that iron boriding case
 120 hardening, diamond-like-carbon (DLC) coating, and tungsten carbide (WC-Co, C2 grade with
 121 submicron WC grains, containing 10 wt.% Co) have significantly higher wear resistance than the
 122 selected tool steels (hardened to HRC 60) that are typically used for knife mill blades, as shown
 123 in Table 1 and Figure S1; therefore, these materials were selected to fabricate candidate blades to
 124 be tested in an actual knife mill. Although iron borided D2 tool steel has very similar abrasion
 125 wear rates as the M2 tool steel, it was selected as a candidate surface treatment due its higher
 126 erosion resistance which was determined via sandblasting testing, (see supplementary Table S1).
 127 Moreover, monolithic D2 tool steel blade was available for iron boriding surface treatment at the
 128 time. Detailed experimental procedure of the loop abrasion wear test as well as sandblasting
 129 results are described in the supplementary. The baseline blades used in the knife mill testing
 130 were made of AISI M2 tool steel. One set of M2 tool steel blades was coated with a ~2 μm thick
 131 DLC coating via plasma-enhanced chemical vapor deposition (PE-CVD, TS NCT, Kennebunk,
 132 ME, USA). Another set of D2 tool steel blades was treated with iron boriding resulting in a ~175
 133 μm hardened layer (IBC Coatings Technologies, Lebanon, IN, USA). The last set of the blades
 134 was assembled with WC-Co inserts (Eberbach Corporation, Belleville, MI, USA).

135 **Table 1.** Properties of the selected blade materials

Blade material	Layer thickness (μm)	Vickers hardness (HV)	Wear rate ($\text{mm}^3/(\text{N}\cdot\text{m})$)
M2 tool steel	-	983 ± 80	$(5.3 \pm 0.16)\times 10^{-4}$
D2 tool steel	-	931 ± 110	$(8.6 \pm 0.66)\times 10^{-4}$
DLC-coated M2 tool steel	~2	1380 ± 268	$(5.3 \pm 0.44)\times 10^{-7}$
Iron-borided D2 tool steel	~150	1569 ± 107	$(5.6 \pm 0.52)\times 10^{-4}$
WC-Co	-	1567 ± 108	$(6.8E \pm 0.84)\times 10^{-5}$

136

137 **2.2. Feedstock material**

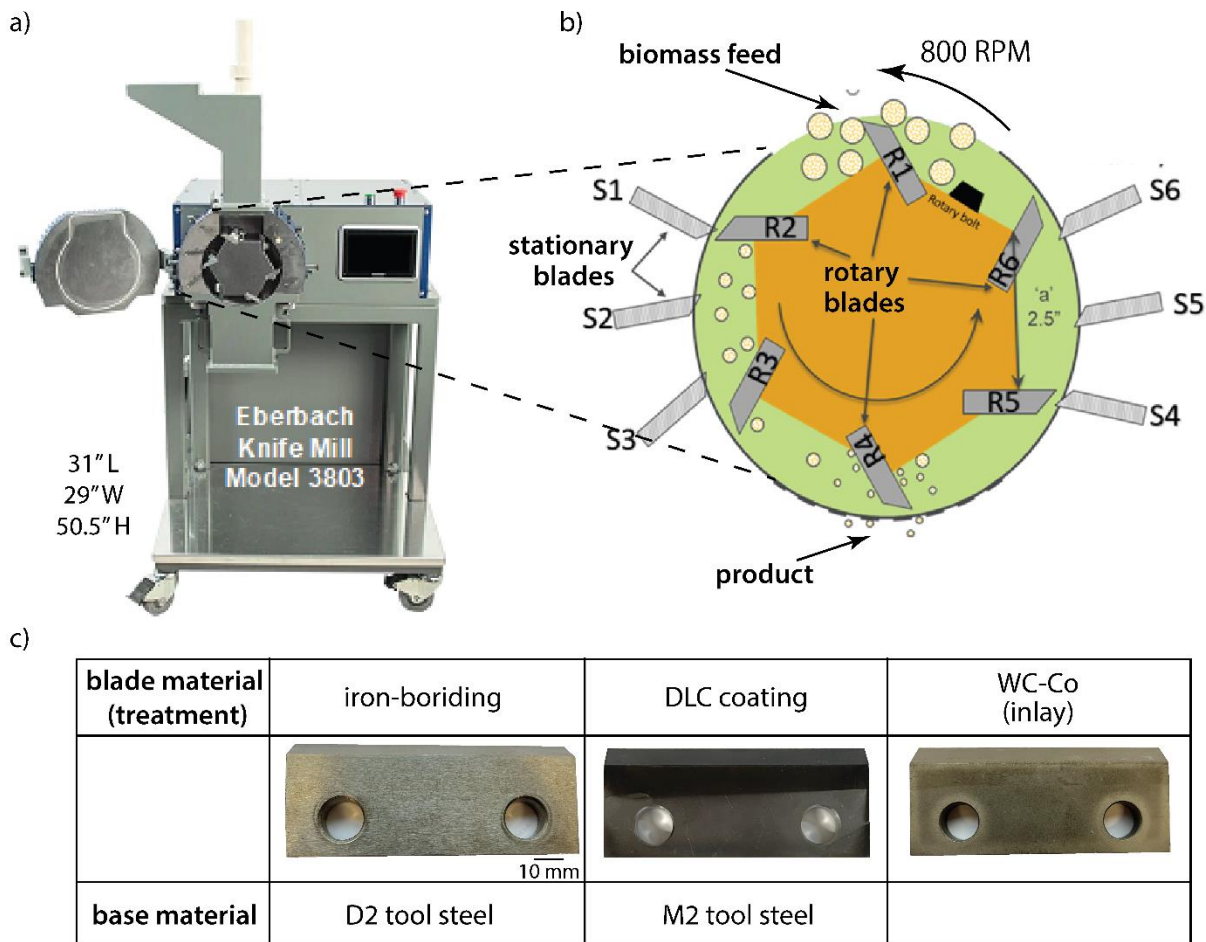
138 The feedstock used for testing was based of material that is common for industrial use.
 139 Loblolly Pine horizontal 2" chipped material used in this study was obtained from FTX
 140 Consulting (Colleton, SC, USA) and stored outdoors until needed. The material was hand sorted
 141 into the following anatomical fractions: needles, bark, twigs/branches, cambium, and white

142 wood. Twigs/branches were smaller in diameter and at least partially covered with bark.
143 Cambium was defined as any wood chip that had a smooth surface where bark was once
144 attached. White wood was defined as wood chips from the interior of the tree. The feedstock was
145 first hammer milled using a $\frac{1}{4}$ inch (6.35 mm) screen and then dried to 11% moisture content
146 before been placed into a super sack. The woodchip particle sizes varied between 0.1 and 4.5
147 mm with an average of 0.7 mm. The detailed particle size distribution is shown in Figure S2. On
148 average, the feedstock contained approximately 8.8 wt.% of ash.

149 **2.3. Knife mill testing**

150 Experimental measurements to determine the wear properties of the candidate blade
151 materials and their milling efficiency were performed on a commercial knife milling unit –
152 Eberbach knife mill Model 3803 (Eberbach Corporation, Belleville, MI, USA), Figure 1. This
153 knife mill configuration consists of six stationary (fixed) blades and six rotary blades mounted on
154 a rotary shaft with a rotational speed of 800 RPM. Size of the screen was 2 mm. During
155 experiment runs feedstock was loaded by rotating through three super sacks of biomass material.
156 Biomass was loaded into a container, weighed and then metered into the grinder using an
157 Eberbach cone feeder (auto feeder). The biomass was fed into the grinder to keep the hoper full
158 and, as a result, different feed rates were observed, as shown in Table 2, because wear-resistant
159 blades allowed higher feed rates. After four hours of run time the mill was stopped, clean, and
160 left to cool down. The total amount of processed feedstock and processing time for each set of
161 blades are shown in Table 2.

162 Three knife mill experiments were conducted, each using a different blade material: M2 tool
163 steel blades with DLC coating, D2 tool steel blades with iron boriding, and WC-Co inserts
164 mounted on tool steel bases. The cutting surface of the blades was approximately 4" (101.6 mm)
165 wide and the cutting tip angle was 51°. Prior to the knife mill testing, each blade was sonicated
166 with RBS 35 Detergent Concentrate (Thermo Scientific, Rockford, IL, USA) and dried in an
167 oven at 80°C overnight.



168

169 **Figure 1.** Experimental setup. a) Knife mill used in the experiments. b) Schematic of a milling
 170 procedure depicting an interaction between stationary, rotary blades and feedstock. c) Images of
 171 the blades.

172 **Table 2.** Total amount of feedstock processed and average feed rate for each blade material in
 173 the knife mill test.

Blade material	Amount of feedstock processed (kg)	Average feed rate (g/min)	Total milling time (hours)
DLC (M2 tool steel)	195	203	16
Iron-borided (D2 tool steel)	197	193	17
WC-Co (tool steel)	218	302	12

174

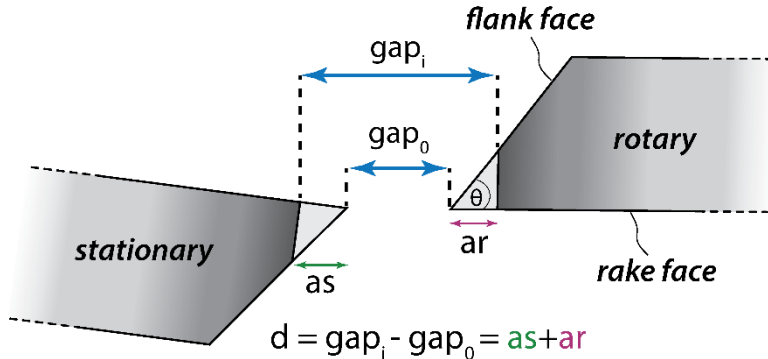
175 2.4. Wear measurements of blades

176 Wear performance of tested blade materials was determined by measuring the evolving gap
 177 between the stationary and rotary blades during knife milling using a feeler gauge, Figure 2. This
 178 method allows to determine the wear (linear) recession of a pair of rotary and stationary blades
 179 by tracking the increasing distance between the opposite blade tips. The gap was measured
 180 between each stationary and rotary blade pair and the resulting gap was determined as an average

181 of a total of 36 measurements (6 stationary blades paired with 6 rotary blades). In order to
 182 determine a relative wear of the blades, the initial gap (gap_o) was measured prior to the testing.
 183 During the milling operation, the knife mill was paused at certain time intervals and the gap
 184 measurement was taken to determine the evolving gap (gap_i). The actual blade edge recession (d)
 185 due to wear is the difference between the evolving gap and the initial gap: $d = gap_i - gap_o$, which
 186 is then converted to a volume loss, V_{loss} as:

$$187 \quad V_{loss} = (ar^2 + as^2) * \tan(\theta) * \frac{w}{2}, \quad (1)$$

188 where ar and as are wear recessions of rotary and stationary blades, respectively, w is the
 189 width of the blade edge and θ is an angle of the blade tip. The values of ar and as in Eq. 1 were
 190 determined as ratios of average volume loss of the rotary, V_r , and stationary, V_s blades,
 191 respectively, over the sum of the average volume loss, $V_r + V_s$, measured with the 3D confocal
 192 microscope in Section 3.1, Figure 5b. More details about the gap measurement calculations are
 193 highlighted in the supplementary.



195 **Figure 2.** Schematic of a recessive gap measurement between a stationary and a rotary blade.

196 The volumetric loss of the blades was also determined by measuring the surface profile of the
 197 tips utilizing 3D laser confocal microscope (Keyence, VK-X1100, Itasca, IL, USA) which is
 198 illustrated in Figure 3. The tip 3D surface topography of all blades was measured before the
 199 milling and after the milling experiments, Figure S3. Five 2D surface profiles were then selected
 200 at five different locations along the blade. The unworn surface profile was aligned with the worn
 201 surface profile of the same blade. The areas of the unworn (A_u) and worn (A_w) blade tips were
 202 calculated by integrating their heights (Z_u) and (Z_w) over the region x . The worn area (A) was
 203 then determined as a difference between the unworn tip area, and the worn tip area:

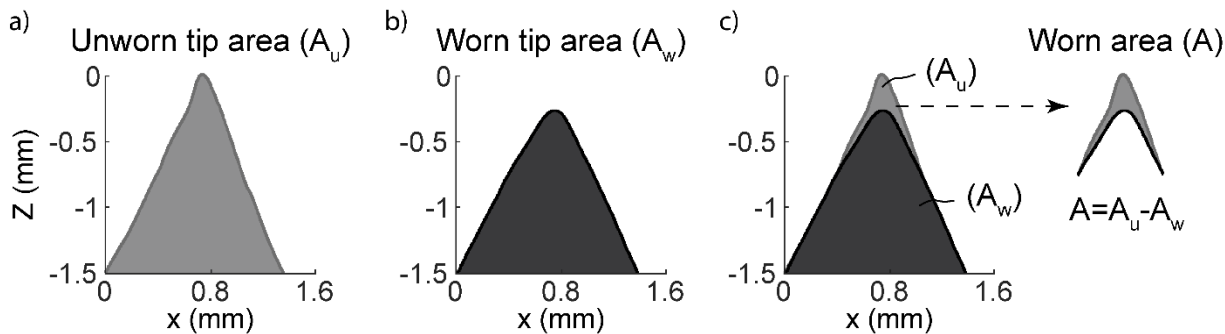
$$204 \quad A = A_u - A_w = \sum Z_u dx - \sum Z_w dx. \quad (2)$$

205 Five worn areas measured along the blade were averaged to estimate the final worn area. The
 206 volume loss was then calculated by multiplying the worn area by the blade width (w):

$$207 \quad V_{loss} = A * w. \quad (3)$$

208

209



210

211 **Figure 3.** Determination of the wear of a M2 standard tool steel blade using 3D laser confocal
 212 microscope. a) Tip area of the middle section of an unworn blade, b) Tip area of the middle
 213 section of a worn blade after the knife mill test. c) Worn blade area determined as the differential
 214 between the unworn and worn blade tips.

215 2.5. Characterization of worn blades

216 The cutting edge, flank and rake faces of the blades were analyzed to identify the wear
 217 modes. Worn blade tips were imaged with optical microscopes (Olympus STM6, Tokyo, Japan;
 218 and Nikon Labophot-2, Tokyo, Japan) and a scanning electron microscope (FEI Quanta 400F,
 219 Hillsboro, OR).

220 2.6. Particle size distribution measurements

221 The evolution of the processed feedstock particle size during knife milling experiments was
 222 measured using a particle size and shape analyzer (Microtrac PartAn3D, Montgomeryville, PA
 223 USA). A dynamic particle analyzer provides a higher resolution and accuracy of a particle size
 224 measurement in comparison to a traditionally used sieve analysis[25]. Samples of processed
 225 feedstock from each of the three knife milling experiments were collected at several intervals: 1
 226 kg, 100 kg and 200 kg of feedstock processed. A threshold of 500 μm was set to filter out
 227 clustered (bundled) particles. The evolution of the particle size distribution is represented via
 228 histograms and as a cumulative distribution.

229 2.7. Milling throughput measurements

230 Throughput, the amount of feedstock processed for a given period, was determined by
 231 monitoring the feedstock mass flow in 40 sec. and 60 sec. intervals. The throughput was
 232 measured for all blade materials during the knife milling experiments.

233 2.8. Techno-economic analysis (TEA)

234 A Discrete Event Simulation (DES) simulation model of the preprocessing system developed
 235 by Hartley et al. [26] was developed and employed to study the economic impact of using the
 236 wear resistant candidate blade materials in a knife mill. The TEA was modeled for an operation
 237 of 4 preprocessing lines, each sized at 600 dry U.S. short tons/day for a total throughput capacity
 238 of 2,400 dry U.S. short tons /day, for a milling period of 350 days, 24 hours/day. Each
 239 preprocessing line utilized four knife mills (JRS 14CHS) consisting of 36 rotating knives and 3
 240 stationary knives each, for a total of 156 blades per preprocessing line (624 total blades in the

241 system). The analysis was based on several inputs and assumptions which are summarized in
 242 Table 3. The cost in 2021\$ of the blade's material was estimated based on inputs from Eberbach
 243 company and surface treatment suppliers. A single standard tool steel blade costs \$350. DLC
 244 coating increases the blade cost by \$8 and iron boriding costs \$15 for treating each blade. A WC-
 245 Co insert costs \$400, which increases the total cost of the knife to \$750 each. The cost of the
 246 blade re-sharpening was estimated to be \$42.50 for the standard tool steel blade or the WC-Co
 247 insert, based on input from a local machine shop. The 're-sharpening' cost of the iron-borided
 248 and DLC-coated blades includes the cost of resharpening the blade substrate and the
 249 reapplication of the surface treatment. The analysis also assumed a complete replacement of the
 250 blades after 3 re-sharpening because of the knife dimension requirements. The downtime cost for
 251 the blade re-sharpening or replacement was estimated to be 40.23 \$/min. The modeled feedstock
 252 cost without knife mill downtime due to knife wear and replacement was 85.07 \$/ton.
 253

254 **Table 3.** Assumptions used in TEA model. Costs shown are in 2021\$.

Blade material	Material cost (\$/blade)	Re-sharpening cost (\$/blade)	Downtime cost (\$/min)	Base feed cost (\$/ton)
M2 tool steel	350	42.50	40.23	85.07
DLC (M2 tool steel)	358	50.50	40.23	85.07
Iron-borided (D2 tool steel)	365	57.50	40.23	85.07
WC-Co (tool steel)	750	42.50	40.23	85.07

255

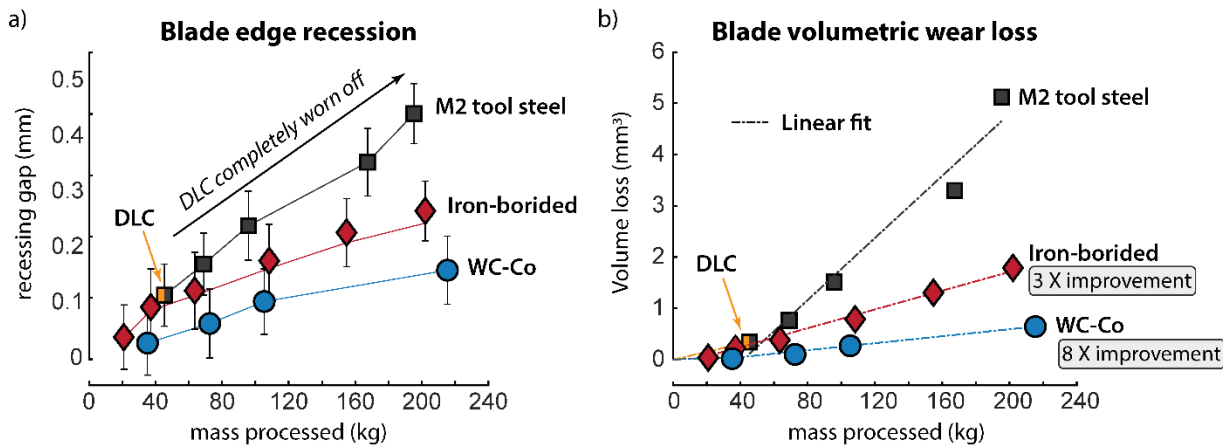
256 **3. Results and Discussion**

257 **3.1. Wear properties of blade materials**

258 Knife milling experiments showed that the WC-Co blades have the highest wear resistance
 259 (the lowest wear rate) among all tested blade materials, as compared in Figure 4. The blade
 260 volumetric wear loss, Figure 4b, was converted from the edge recession measurements, Figure
 261 4a, using Eq. 1. At the end of the test, after ~220 kg of feedstock processed, the total volumetric
 262 loss of the WC-Co blade was ~0.65 mm³ which is ~8 and ~2.5 times lower than that of the iron-
 263 borided blade, ~1.79 mm³, Figure 4b. Both WC-Co and iron-borided blades exhibit a linear
 264 relationship between the blade volumetric loss and the amount of feedstock processed although
 265 the iron-borided blade had a slightly higher run-in wear, the initial ~40 kg of feedstock
 266 processed, Figure 4a.

267 In contrast, the DLC-coated tool steel blades performed poorly. Although the bench-scale
 268 wear testing suggested a high wear resistance for the DLC coating, Table 1 and Figure S1, the
 269 coating on the blade tip was worn off quickly, after less than 50 kg of feedstock processed, based
 270 on visual inspection. By that moment, the DLC-coated blades had a similar wear rate to the iron-
 271 borided ones, which could be contributed to the DLC coating being partly present during that
 272 period. Since the blade tip was not protected by the DLC coating afterwards, the measured blade
 273 edge recessions and volumetric losses were assigned to the M2 tool steel substrate, which is used
 274 as the baseline in this work. A linear fit was made through all the volumetric loss data points of
 275 each blade material to determine the wear rate expressed as blade volumetric loss over amount of

276 feedstock processed [mm³/kg], Figure 4b. Remarkably, WC-Co had 8X lower wear rate than the
 277 standard tool steel while the iron-borided blade reduced the wear rate by 3X, as detailed in Table
 278 4.



279
 280 **Figure 4.** Wear performance of the three different sets of blades in the knife mill tests. a)
 281 Average recessing gaps of the blade tips over the amount of feedstock processed. b) Average
 282 volume losses of the blade tips converted from the recessing gaps over the amount of feedstock
 283 processed.

284

285 **Table 4.** Wear rates of blade materials in the knife mill tests.

Blade material	Wear rate (mm ³ /kg)	Wear rate improvement (%)
*M2 tool steel	3.0×10^{-2}	baseline
Iron-borided D2 tool steel	9.1×10^{-3}	230
WC-Co	3.6×10^{-3}	730

286 *Note: wear rate of M2 tool steel after DLC coating was worn off.

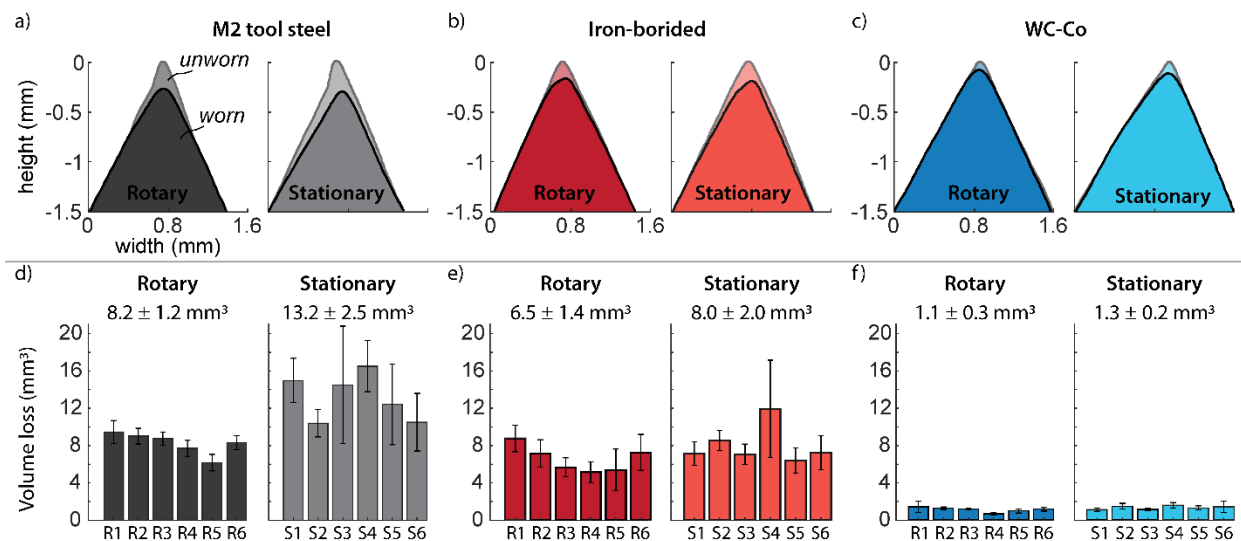
287

288 Comparison of unworn and worn surface profiles of the middle sections of selected
 289 stationary and rotary blades in Figure 5 and supplementary Figure S5, showed similar trends that
 290 were observed from the gap recession measurements in Figure 4. WC-Co blades had the lowest
 291 worn area followed by the iron-borided blade and the standard M2 tool steel blade, Figure 5(a-c).
 292 The volume loss of the blade tips of all tested knives determined from the worn area
 293 measurements, Eq. 2, is shown in Figure 5(d-f).

294 The trends in the volumetric loss of the blades are the same as those from the gap
 295 measurements, however, the values do not match, which is due to the differences in the
 296 measurement techniques. The calculation of the volumetric loss from the gap measurements
 297 intends to underestimate the wear because it does not include the wear on the flank and rake
 298 faces. Also, the edge chipping was 'overlooked' by the gap measurement because the feeler
 299 gauge touched on the tallest point.

300 Interestingly, both worn surface profiles and volumetric loss results suggest that the
 301 stationary blades worn more than the rotary blades for all three blade materials, Figure 5b. This
 302 trend is especially apparent in M2 tool steel blades in which the stationary blades had ~60%
 303 higher volumetric loss than the rotary blades. The abrasive wear of the rotary and stationary
 304 blades would be about the same because of the symmetry of the relative motion and force at the
 305 contact interface. Therefore, it is the erosion that made the difference between the rotary and
 306 stationary blades. If a particle has an elastic collision against a rotary blade, both the momentum
 307 and mechanical energy are preserved. Therefore, the velocity of the inorganic particle after a
 308 collision with the rotary blade would be roughly 2x of the velocity of the rotary blade (see
 309 derivation in Section 2 of the Supporting Information). If a particle has a perfect inelastic
 310 collision against a rotary blade, only the momentum is preserved and the particle would be stick
 311 onto the blade. As a result, the velocity of the particle would be same as the velocity of the rotary
 312 blade. Therefore, the velocity of a particle impacting a stationary blade would always be higher
 313 than a rotary blade speed. This explains why more wear was on the stationary blades than on the
 314 rotary blades.

315



316 **Figure 5.** Wear of the blade tips measured with a 3D laser confocal microscope. Comparison of
 317 unworn and worn tips of the middle section of selected blades of a) M2 tool steel, b) Iron-
 318 borided knives, and c) WC-Co knives. Volumetric loss of the blades of knives d) M2 tool steel
 319 knives, e) Iron-borided knives, and f) WC-Co knives.

321

322 3.2. Worn blade morphology

323 Analysis of the worn blade tips after completion of the knife mill testing revealed underlying
 324 different wear mechanisms for the three blade materials, as shown in Figure 6 and Figure 7. The
 325 DLC coating was worn off from M2 tool steel baseline due to abrasion which is evident from the
 326 images of the flank face, rake face and cutting edge of the blade, Figure 6(a-c). The transition

327 from the area covered by the residual DLC coating to the substrate exposed area on the rake face
328 is relatively smooth without evidence of cracking or delamination, which indicates that the DLC
329 coating on the blade tip was likely removed by abrasion and/or erosion instead of fracture or
330 spallation, Figure S4.

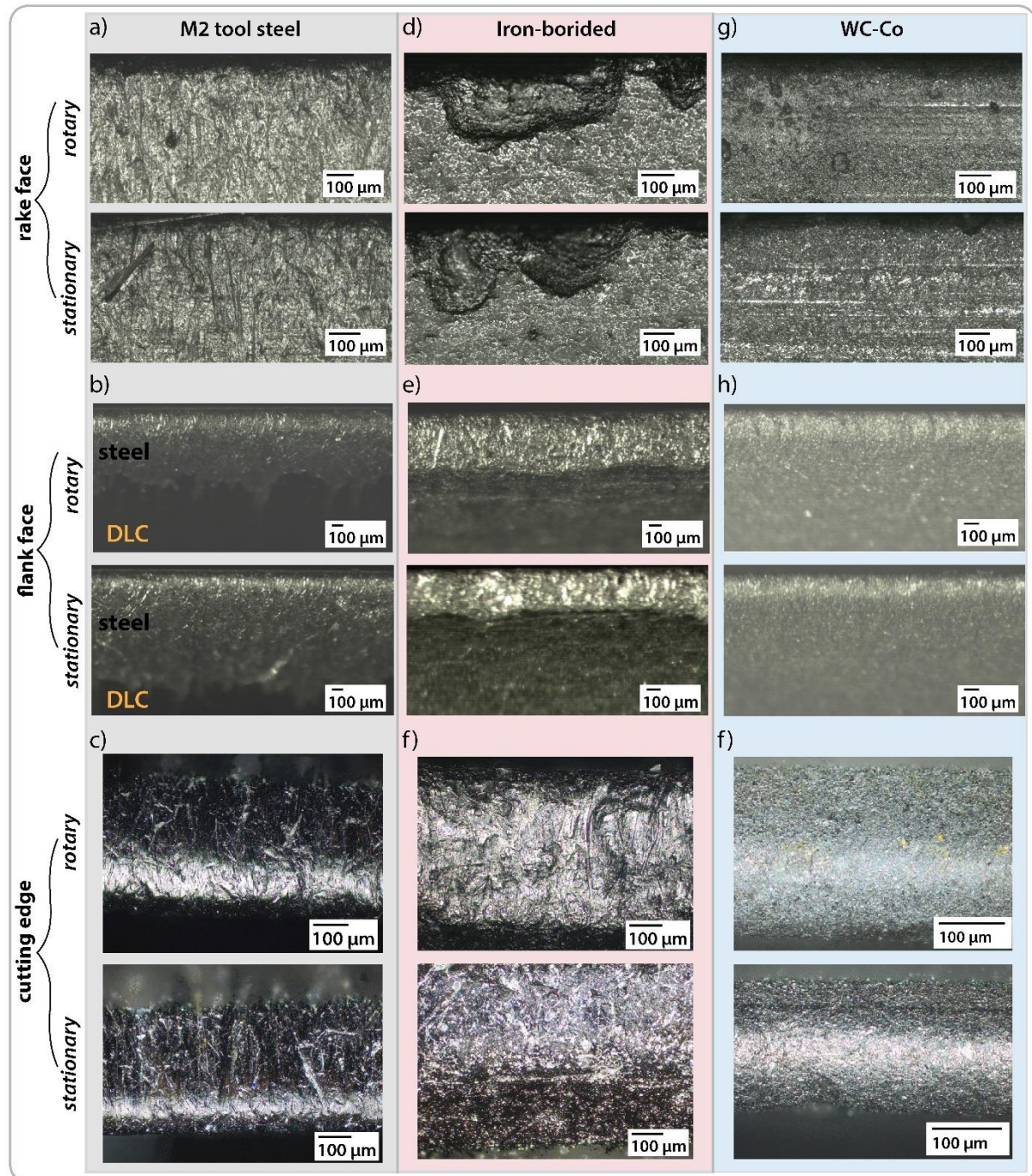
331 The wear modes of the substrate M2 tool steel (after DLC removal) are erosion on the rake
332 face, Figure 6a, and abrasive wear on the flank face and cutting edge, Figure 6(b,c). The degree
333 of wear of the rotating blade appears to be less severe than that of the stationary blade, Figure
334 6(a-c). In addition, cross-sectional SEM examination revealed a pronounced subsurface crack
335 near the cutting edge of a stationary blade, which may be attributed to repeatable impact with the
336 biomass feedstock leading to fatigue failure, Figure 7c.

337 The rake face of both the stationary and rotary iron-borided blades had significant chipping
338 as a result of erosion near the tip, Figure 6d and Figure 7(d,e). The optical image, Figure 6e, of
339 the flank face of the rotating blade shows evidence of abrasive wear in a form of pronounced
340 scratches. The cutting edge in the borided blade shows pitting of the surface layer at different
341 scales, Figure 6f. Similar to the M2 tool steel blade, a possibly fatigue-induced subsurface crack
342 was also observed just below the cutting edge of the iron-borided D2 tool steel blade (still in the
343 zone of iron boriding), Figure 7f.

344 WC-Co blades had the lowest surface damage. The optical images show much less
345 significant erosion with a smaller-scale pitting and chipping on the rake face, Figure 6g, and
346 abrasion with shorter and shallower scratches on the flank face, Figure 6h, compared with the
347 iron-borided blades. The SEM images, Figure 7(g-i), revealed that WC-Co particles are extruded,
348 removed or pushed away by erosion, micro-fracture and chipping of the WC-Co grains.

349

350

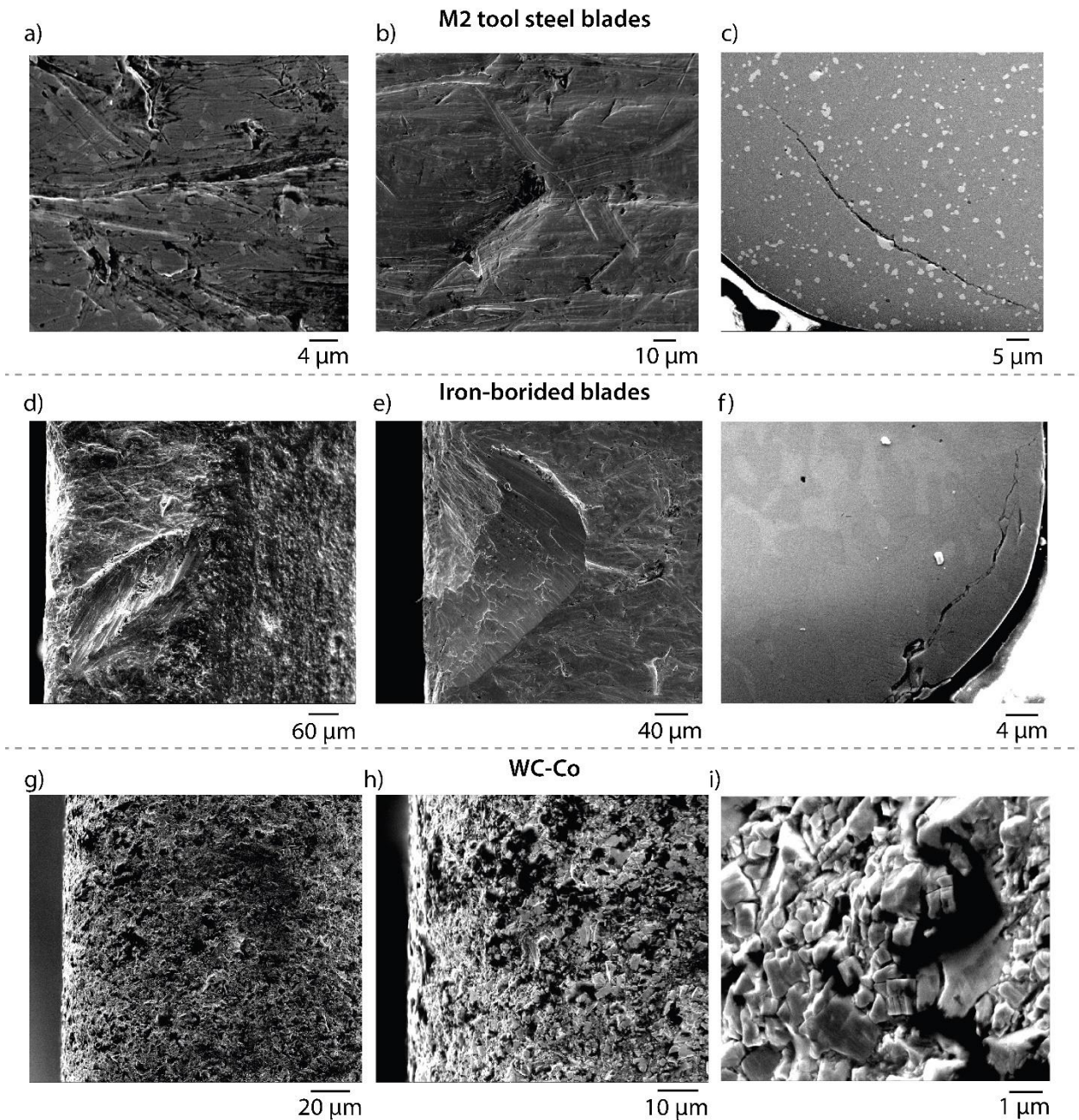


351

352 **Figure 6.** Optical images of worn blade tips of (a-c) DLC-coated M2 tool steel, (d-f) Iron-
 353 borided D2 tool steel, (g-f) WC-Co.

354

355



356

357 **Figure 7.** SEM images of worn blade tips. (a-c) M2 tool steel. (d-f) Iron borided. (g-i) WC-Co.

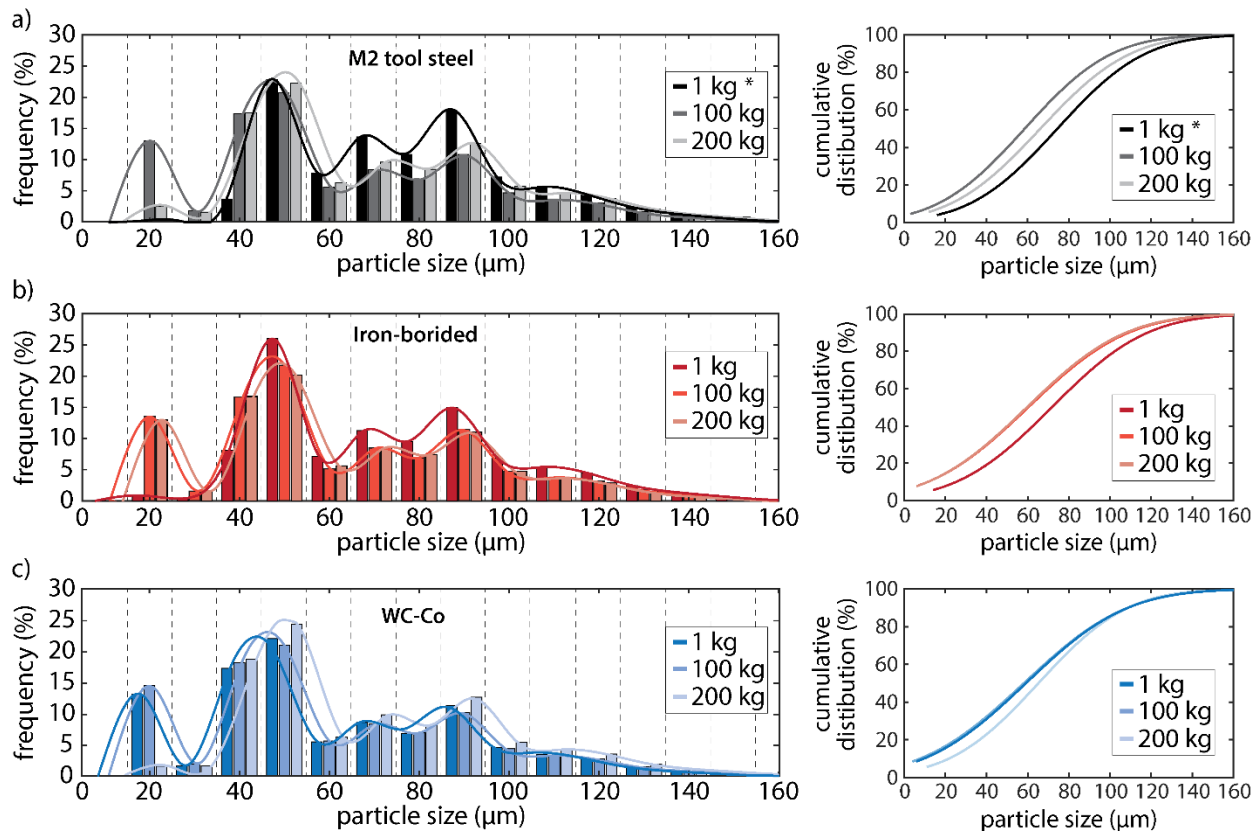
358

359 **3.3. Particle size distribution**

360 A comprehensive particle size analysis revealed that the biomass particle sizes after the knife
 361 mill testing are in a range of 10 – 160 μm , Figure 8. While the overall particle size distributions
 362 (PSDs) appear to be similar for the three blade materials, some differences were observed. For
 363 the M2 tool steel, the initial 1 kg of feedstock processed likely corresponds to the DLC coating
 364 before it being worn off. As expected, milling with worn blades (after 100 kg and 200 kg of

365 feedstock processed) resulted in more smaller particles ($<50 \mu\text{m}$) but less medium sized particles
 366 ($50\text{--}120 \mu\text{m}$) for the M2 tool steel and iron-borided blades, Figure 8 (a,b). This is because worn
 367 blades would rely more on impact-induced fracture than on cutting in the particle size reduction.
 368 Such a trend was not present for the WC-Co blades, instead Figure 8c shows little change in PSD
 369 after 1, 100, or 200 kg of feedstock processing. This suggests that the blades were still sharp and
 370 cutting the woodchips effectively by the end of the knife mill test, which can be confirmed by the
 371 blade morphology in Figure 6 above.

372



373

374 **Figure 8.** Evolution of particle size distribution and cumulative distribution for blades of a) M2
 375 tool steel (*initial 1 kg of feedstock processed with the DLC coating before being worn off), b)
 376 Iron-borided, and c) WC-Co.

377

378 3.4. Knife milling feedstock throughput and power consumption

379 Figure 9a compares the throughput during the knife mill tests of the three sets of blades.
 380 Throughput was determined by measuring the amount of feedstock processed over a certain time
 381 interval. The more wear-resistant WC-Co and iron-borided blades evidently increased the
 382 throughput. By the end of the test, the throughput for these two wear-resistant blades was around
 383 5-6 g/s, about three times higher than that ($<2 \text{ g/s}$) for the M2 steel blades. This could be
 384 attributed to the improved wear resistance that better retained the sharpness of the blades.

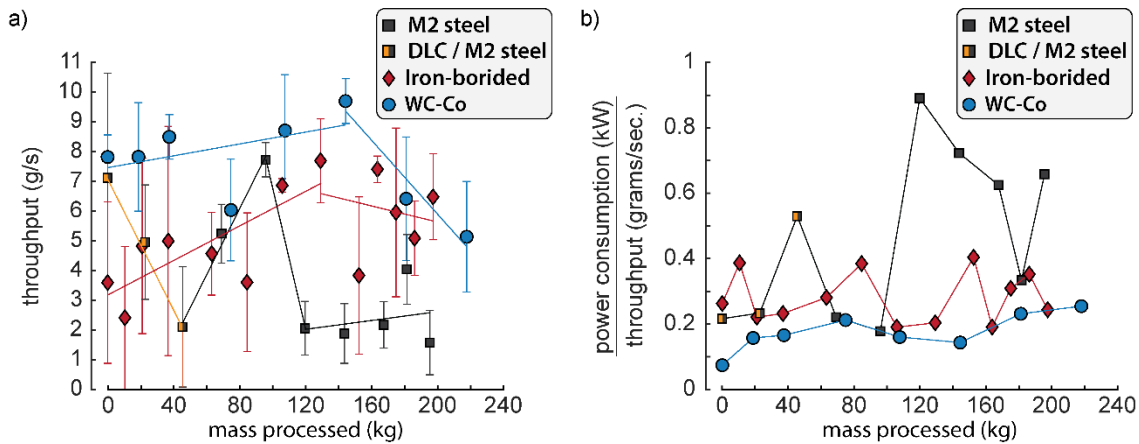
385 The throughput was expected to start at the highest level at the beginning of milling when the
 386 blades are the sharpest and the blade gaps are the smallest, and then gradually decrease with the
 387 amount of feedstock processed due to wear. However, except the throughput for the DLC coated
 388 blades showed a quick drop before the coating was worn out (0-40 kg), the throughputs had an
 389 increasing trend initially for the iron-borided (0-130 kg) and WC-Co (0-140 kg) blades as well as
 390 for the M2 steel blades right after the DLC coating was removed (45-95 kg), as shown in Figure
 391 9a. This is counter-intuitive. It is hypothesized that the increase in throughput was due to
 392 chipping of the blade cutting edge as observed in Figure 6 (a,d,g). Chipping could actually
 393 increase the localized contact pressure against the feedstock to provide more efficient size
 394 reduction. In the meantime, the cutting edge was becoming thicker or blunter due to abrasive
 395 wear. Therefore, edge chipping and thickening, each as part of the blade wear process, were
 396 likely competing in determining the throughput. Based on that, the throughput may be
 397 categorized into three stages during the knife mill test: (Stage 1) throughput initially rose because
 398 edge chipping increased the contact pressure against the feedstock outweighing the edge
 399 thickening (blunting), (Stage 2) throughput decreased when edge chipping became less
 400 significant because the edge was getting thicker and its effect was overshadowed by blunting,
 401 and (Stage 3) throughput dropped to a trendless lower level when the gap between the rotary and
 402 stationary blades was so large that the milling process was no longer sensitive to the edge
 403 sharpness. Linear fits were made through the data points in each stage to highlight the trends.

404 From Figure 9a, it appears that the M2 steel blades already reached the third stage because of
 405 their higher wear rates, but the iron-borided and WC-Co blades were still in the second stage by
 406 the end of the tests. The initial throughput for the DLC-coated M2 tool steel blades was ~7 g/sec
 407 and decreased to ~2 g/sec by the time the coating was worn off (~45 kg feedstock). The
 408 throughput of the uncoated M2 tool steel blades initially increased to ~7.5 g/sec (Stage 1, 45-95
 409 kg) but then quickly decreased to ~2 g/sec after processing ~120 kg feedstock (Stage 2) and
 410 maintained at that level to the end of the test (Stage 3). The WC-Co blades started with a high
 411 throughput of ~8 g/sec and slowly increased to ~9 g/sec after processing ~140 kg feedstock
 412 (Stage 1), and then saw the throughput decreasing to ~5 g/sec by the end of the test (Stage 2).
 413 The iron-borided blades started with a lower throughput, ~3 g/sec, compared with other blades.
 414 A possible reason is that the substrate steel blades went through a blasting process to remove
 415 surface oxides in preparation for iron boriding and thus were not as sharp as other two types of
 416 blades. The throughput for the iron borided blades increased along with the amount of feedstock
 417 processed and reached a peak of ~7.5 g/sec after processing ~130 kg feedstock (Stage 1) and
 418 slowly decreased to 5-6 g/sec by the end of the test (Stage 2).

419 Power consumption was recorded during each knife mill test (excluding the periods when the
 420 knife mill was paused or no biomass feedstock was fed). It is understood that the recorded power
 421 consumption counts both the active power used for feedstock size reduction and all the passive
 422 resistances that unfortunately could not be easily separated. The power consumption is also
 423 directly related to the throughput, and thus the measured power consumption was normalized by
 424 the corresponding throughput (kW/(g/sec)), basically the energy consumed per unit feedstock
 425 mass, Figure 9b. The results clearly demonstrate that the normalized power consumption was
 426 lower with the improved wear resistance of the blades. Normalized power consumption of knife

427 milling operation using the WC-Co blades was not only the lowest among all blade materials but
 428 also the most consistent. In contrast, the normalized power consumption was on average the
 429 highest and the most inconsistent when using the standard tool steel blades.

430



431

432 **Figure 9.** Knife milling performance using different blade materials. a) Feedstock throughput
 433 during the test; b) Power consumption normalized by throughput during the test.

434

435 3.5. Techno-economic analysis (TEA)

436 The knife milling results were used as inputs in a TEA, as illustrated in Figure S6, to
 437 demonstrate the economic feasibility of replacing the standard tool steel blade with the more
 438 wear resistant WC-Co or iron-borided blades. The TEA results are summarized in Table 5. This
 439 analysis consists of several assumptions which are listed in Table 3. Certain inputs are
 440 independent to the blade material such as downtime cost or base feedstock cost. The most
 441 important inputs are those that are material-specific which are the blade cost, blade re-sharpening
 442 cost, and blade durability. The cost of the knife milling using different blade materials was
 443 simulated for a system of four preprocessing lines, each containing four full-size commercial
 444 knife mills (JRS 14CHS) with each mill consisting of 39 knives (36 rotating knives and 3
 445 stationary knives) for a period of 350 days (50 weeks), 24 hours/day. First, it is imperative to
 446 determine the number of failures for different blade materials. In this analysis, a failure means a
 447 blade requires re-sharpening or replacement due to wear. When the blades are re-sharpened 3
 448 times, they will be replaced by a new set. Based on the field experiences with knife mill
 449 operation, the standard tool steel blades need to be resharpened after 100 tons of ash had passed
 450 through the mill (estimated from the vendor, Rawlings Manufacturing, Missoula, MT, USA per
 451 personal communication). Applying iron-boriding surface treatment and WC-Co inlay would
 452 enable the blades to process 326 and 746 tons of ash, respectively, before replacing them, Figure
 453 S7. This finding is especially important for knife milling dirty biomass with a high content of
 454 ash. Improving the wear resistance of the blades allows to process larger amount of ash which
 455 would decrease the downtime associated with less frequent replacement of the blades. More
 456 detailed information about TEA can be found in the supplementary.

457 For the tool steel DES simulation (with stochastically-sampled ash contents from a
 458 distribution), this resulted in failures roughly every 2 weeks which is an equivalent of
 459 approximately 104 failures in a 50-week period for the 4 sets of four knife mills (Table 5). The
 460 improvement in the tool life for the other blade materials is based on the knife mill testing results
 461 in Table 4. The reduced number of modeled failures were 32 and 12 for the iron-borided and
 462 WC-Co blades, respectively. The reduction in the blade failures automatically increased the
 463 amount of produced feedstock and decreased the downtime. The highest reduction of the
 464 downtime cost per amount of biomass pre-processed is achieved with the WC-Co blades ~ 0.20
 465 \$/ton, which is significantly lower than the downtime cost using the standard blades, 1.37 \$/ton.
 466 The downtime cost for the iron-borided blades was determined to be 0.47 \$/ton. Lower
 467 frequency of the blade failures also reduces their overall cost. Re-sharpening and replacing WC-
 468 Co blades would cost only \$1.10 per ton of biomass pre-processed and \$1.84 with iron-borided
 469 blades. This is significantly lower than the cost of the standard blades, \$4.22. The total milling
 470 cost determined as a sum of knife cost, downtime cost and feedstock cost was the highest for the
 471 M2 tool steel blades, 75.71 \$/ton, followed by the iron-borided blades, 72.44 \$/ton and the WC-
 472 Co blades, 71.42 \$/ton. The analysis clearly demonstrates that the knife milling operation cost is
 473 notably reduced by applying more wear-resistant blade materials.

474

475 **Table 5.** TEA of different blade materials simulated for an operation of four sets of four knife
 476 mills (total 16 mills) each containing 39 knives based on knife mill testing results.

Blade material	Initial knife cost (\$)	# of failures	Biomass produced (ton)	Downtime (min)	Knife cost (\$/ton)	Total cost (\$/ton)
M2 tool steel	54,600	104	486,052	16,672	4.22	75.71
Iron-borided D2 tool steel	56,940	32	486,832	5,760	1.84	72.44
WC-Co inlay + tool steel	117,000	12	499,048	2,496	1.10	71.42

477

478 4. Conclusions

479 This study demonstrates that applying wear resistant blade materials can significantly
 480 enhance the durability and performance of a knife mill for biomass pre-processing. The knife
 481 wear rate, worn blade morphology, biomass particle size distribution, feedstock throughput, and
 482 power consumption were measured for three different blade materials: DLC-coated M2 tool
 483 steel, iron-borided D2 tool steel, and tungsten carbide-cobalt composite. Knife milling
 484 experiments showed that the tungsten carbide inserts provided 8X wear performance
 485 improvement, followed by iron-boriding surface treatment with a 3X wear reduction when
 486 compared to the commonly used tool steel blades. In contrast, the thin DLC coating was worn off
 487 quickly and thus is not suitable for the knife mill application. The improved durability of
 488 tungsten carbide blades is attributed to a high resistance against both erosion and abrasion while
 489 the iron-borided blades showed significant edge chipping and spalling. The enhancement in the

490 wear resistance of the blades also resulted in a higher throughput and a lower normalized power
 491 consumption, but had less impact on the particle distribution of the processed biomass. Techno-
 492 economic analysis predicts that using the tungsten carbide or iron-borided blades could
 493 potentially reduce the overall operational cost of a knife mill despite their higher cost when
 494 compared to the standard tool steel blades.

495

496

497 Acknowledgements

498 The authors would like to thank Drs. E. Wolfrum from NREL, L. Lin and J. Keiser from ORNL,
 499 V. Thompson from INL, and P. Blau from Blau Tribology Consulting for their thoughtful
 500 comments in technical discussion. The authors would also like to acknowledge Dr. C. Lorenzo-
 501 Martin from ANL for SEM imaging of selected worn blades. The research was sponsored by the
 502 Feedstock-Conversion Interface Consortium (FCIC) of the Bioenergy Technologies Office,
 503 Office of Energy Efficiency and Renewable Energy (EERE), US Department of Energy (DOE).

504 *Notice: This manuscript has been authored by UT-Battelle, LLC and Battelle Energy Alliance,
 505 LLC, under contracts DE-AC05-00OR22725 and DE-AC07-05ID14517 with the US Department
 506 of Energy (DOE). The US Government retains and the publisher, by accepting the article for
 507 publication, acknowledges that the US government retains a nonexclusive, paid-up, irrevocable,
 508 worldwide license to publish or reproduce the published form of this manuscript, or allow others
 509 to do so, for US government purposes. DOE will provide public access to these results of
 510 federally sponsored research in accordance with the DOE Public Access Plan
 511 (<http://energy.gov/downloads/doe-public-access-plan>).*

512

513

514 References

- 515 [1] M.-A. Perea-Moreno, E. Samerón-Manzano, and A.-J. Perea-Moreno, "Biomass as Renewable
 516 Energy: Worldwide Research Trends," *Sustainability*, vol. 11, no. 3, p. 863, Feb. 2019, doi:
 517 10.3390/su11030863.
- 518 [2] A. Tursi, "A review on biomass: importance, chemistry, classification, and conversion," *Biofuel
 519 Research Journal*, vol. 6, no. 2, pp. 962–979, Jun. 2019, doi: 10.18331/BRJ2019.6.2.3.
- 520 [3] J. Cheng, *Biomass to renewable energy processes*. CRC press, 2017.
- 521 [4] T. Bridgwater, "Biomass for energy," *J Sci Food Agric*, vol. 86, no. 12, pp. 1755–1768, Sep. 2006,
 522 doi: 10.1002/jsfa.2605.
- 523 [5] S. V. Vassilev, D. Baxter, L. K. Andersen, and C. G. Vassileva, "An overview of the chemical
 524 composition of biomass," *Fuel*, vol. 89, no. 5, pp. 913–933, 2010, doi: 10.1016/j.fuel.2009.10.022.
- 525 [6] O. Oyedeleji, P. Gitman, J. Qu, and E. Webb, "Understanding the Impact of Lignocellulosic Biomass
 526 Variability on the Size Reduction Process: A Review," *ACS Sustain Chem Eng*, vol. 8, no. 6, pp.
 527 2327–2343, Feb. 2020, doi: 10.1021/acssuschemeng.9b06698.
- 528 [7] Z. Miao, T. E. Grift, and K. C. Ting, "Size Reduction and Densification of Lignocellulosic Biomass
 529 Feedstock for Biopower, Bioproducts, and Liquid Biofuel Production," in *Encyclopedia of*

530 *Agricultural, Food, and Biological Engineering, Second Edition*, CRC Press, 2010, pp. 1–4. doi:
531 10.1081/E-EAFE2-120051298.

532 [8] L. Kratky and T. Jirout, “Biomass Size Reduction Machines for Enhancing Biogas Production,”
533 *Chem Eng Technol*, vol. 34, no. 3, pp. 391–399, 2011, doi: 10.1002/ceat.201000357.

534 [9] L. J. Naimi, “A study of cellulosic biomass size reduction,” *Thesis, University of British Columbia*,
535 2016, doi: doi.org/10.14288/1.0224813.

536 [10] S. Roy, K. Lee, J. A. Lacey, V. S. Thompson, J. R. Keiser, and J. Qu, “Material Characterization-
537 Based Wear Mechanism Investigation for Biomass Hammer Mills,” *ACS Sustain Chem Eng*, vol. 8,
538 no. 9, pp. 3541–3546, Mar. 2020, doi: 10.1021/acssuschemeng.9b06450.

539 [11] J. H. Lee, J. H. Kwon, T. H. Kim, and W. Il Choi, “Impact of planetary ball mills on corn stover
540 characteristics and enzymatic digestibility depending on grinding ball properties,” *Bioresour
541 Technol*, vol. 241, pp. 1094–1100, 2017, doi: <https://doi.org/10.1016/j.biortech.2017.06.044>.

542 [12] A. S. da Silva, H. Inoue, T. Endo, S. Yano, and E. P. S. Bon, “Milling pretreatment of sugarcane
543 bagasse and straw for enzymatic hydrolysis and ethanol fermentation,” *Bioresour Technol*, vol.
544 101, no. 19, pp. 7402–7409, Oct. 2010, doi: 10.1016/j.biortech.2010.05.008.

545 [13] J. M. S. Eng, K. Km, and H. Motjotji, “The Effect of Ball Size Diameter on Milling Performance,”
546 *Journal of Material Science & Engineering*, vol. 04, no. 01, pp. 4–6, 2014, doi: 10.4172/2169-
547 0022.1000149.

548 [14] K. Lee, D. Lanning, L. Lin, E. Cakmak, J. R. Keiser, and J. Qu, “Wear Mechanism Analysis of a New
549 Rotary Shear Biomass Commminution System,” *ACS Sustain Chem Eng*, vol. 9, no. 35, pp. 11652–
550 11660, Sep. 2021, doi: 10.1021/acssuschemeng.1c02542.

551 [15] S. Mani, L. G. Tabil, and S. Sokhansanj, “Grinding performance and physical properties of wheat
552 and barley straws, corn stover and switchgrass,” *Biomass Bioenergy*, vol. 27, no. 4, pp. 339–352,
553 2004, doi: 10.1016/j.biombioe.2004.03.007.

554 [16] S. Paulrud, J. E. Mattsson, and C. Nilsson, “Particle and handling characteristics of wood fuel
555 powder: effects of different mills,” *Fuel Processing Technology*, vol. 76, no. 1, pp. 23–39, Apr.
556 2002, doi: 10.1016/S0378-3820(02)00008-5.

557 [17] V. S. P. Bitra, A. R. Womac, C. Igathinathane, and S. Sokhansanj, “Knife Mill Commminution Energy
558 Analysis of Switchgrass, Wheat Straw, and Corn Stover and Characterization of Particle Size
559 Distributions,” *Trans ASABE*, vol. 53, no. 5, pp. 1639–1651, 2010, doi: 10.13031/2013.34886.

560 [18] L.J. Naimi, S. Sokhansanj, X. Bi, C. J. Lim, A. R. Womac, A. K. Lau, S. Melin, “Development of Size
561 Reduction Equations for Calculating Energy Input for Grinding Lignocellulosic Particles,” *Appl Eng
562 Agric*, vol. 29, no. 1, pp. 93–100, 2013, doi: 10.13031/2013.42523.

563 [19] J. A. Lacey, J. E. Aston, S. Hernandez, M. Intwan, V. S. Thompson, K. Lee, J. Qu, “Wear and Why?
564 How Ash Elements Can Help Define Wear Profiles of Biomass Feedstocks,” 2019. doi:
565 10.13031/aim.201901446.

566 [20] J. A. Lacey, J. E. Aston, and V. S. Thompson, "Wear Properties of Ash Minerals in Biomass," *Front*
567 *Energy Res*, vol. 6, no. NOV, pp. 1–6, Nov. 2018, doi: 10.3389/fenrg.2018.00119.

568 [21] Z. Chen, G. Yu, X. Yuan, Q. Wang, and J. Kan, "Improving the Conventional Pelletization Process to
569 Save Energy during Biomass Densification," *Bioresources*, vol. 10, no. 4, pp. 6576–6585, Aug.
570 2015, doi: 10.15376/biores.10.4.6576-6585.

571 [22] R. M. Singh, "Study on Wearing of Screw of Biomass Briquetting Extruder," *Nepal Journal of*
572 *Science and technology Vol 2*, no. October, pp. 83–86, 2000.

573 [23] K. Lee, S. Roy, E. Cakmak, J. A. Lacey, T. R. Watkins, H. M. Meyer, V. S. Thompson, J. R. Keiser, J.
574 Qu, "Composition-Preserving Extraction and Characterization of Biomass Extrinsic and Intrinsic
575 Inorganic Compounds," *ACS Sustain Chem Eng*, vol. 8, no. 3, pp. 1599–1610, Jan. 2020, doi:
576 10.1021/acssuschemeng.9b06429.

577 [24] "ASTM G 174 Standard test method for measuring abrasion resistance of materials by abrasive
578 loop contact," *ASTM Annual Book of Standards*, vol. 3, pp. 735–739, 2014, doi: 10.1520/G0174-
579 04R17.

580 [25] H. Wei, T. Zhao, Q. Meng, X. Wang, and B. Zhang, "Quantifying the Morphology of Calcareous
581 Sands by Dynamic Image Analysis," *International Journal of Geomechanics*, vol. 20, no. 4, Apr.
582 2020, doi: 10.1061/(ASCE)GM.1943-5622.0001640.

583 [26] D. S. Hartley, D. N. Thompson, L. M. Griffel, Q. A. Nguyen, and M. S. Roni, "Effect of Biomass
584 Properties and System Configuration on the Operating Effectiveness of Biomass to Biofuel
585 Systems," *ACS Sustain Chem Eng*, vol. 8, no. 19, pp. 7267–7277, May 2020, doi:
586 10.1021/acssuschemeng.9b06551.

587